J|A|C|S
COMMUNICATIONS

Published on Web 03/09/2006

Multifunctional Polymeric Nanoparticles from Diverse Bioactive Agents

Paul A. Bertin,[†] Julianne M. Gibbs,[†] Clifton Kwang-Fu Shen,[†] C. Shad Thaxton,[†] William A. Russin,[‡] Chad A. Mirkin,[†] and SonBinh T. Nguyen*,[†]

Department of Chemistry and International Institute for Nanotechnology, Biological Imaging Facility and Department of Neurobiology and Physiology, Northwestern University, Evanston, Illinois 60208-3113

Received September 16, 2005; E-mail: stn@northwestern.edu

Reliable strategies for constructing multifunctional nanomaterials are central to the emerging field of bionanotechnology.[1−6] In particular, it is anticipated that nanostructures which combine the unique functions of diverse bioactive agents will enable future breakthroughs in biomedical research.[7] To this end, we employed ring-opening metathesis polymerization (ROMP) to prepare amphiphilic block copolymers containing small-molecule drug segments (>50% w/w) and tosylated hexaethylene glycol segments and assembled them into core−shell polymeric nanoparticles (PNPs) that allowed for the surface conjugation of single-stranded DNA sequences and/or tumor-targeting antibodies (Scheme 1). To endow our PNPs with biomolecules relevant to breast cancer, we modified them with Bcl-2 antisense oligodeoxynucleotides (asODNs)[8] and antibodies that target the transmembrane human epidermal growth factor receptor-2 (HER-2).[9]

Previously, we employed ROMP to construct nanoparticles with core−shell-type architectures that incorporated high densities of indomethacin[10] or the anticancer drug doxorubicin,[11] which were released in acidic environments relevant to those observed in tumor tissues. In the present system, we prepared an amphiphilic block copolymer (M_n = 30 kDa/mol, M_w/M_n = 1.13), denoted $\mathbf{1}_{35}-b-\mathbf{2}_{15}$, from indomethacin-containing norbornene (**1**)[10] and a tosylated hexaethylene glycol-containing norbornene (**2**) by stepwise block copolymerization. Dynamic light scattering of PNPs assembled in water from $\mathbf{1}_{35}-b-\mathbf{2}_{15}$ revealed particles with effective hydrodynamic diameters (D_H) of 170 ± 30 nm and corresponding polydispersity factors of 0.04 ± 0.03. Observation of these nanoparticles in the solid state by transmission electron microscopy (TEM) confirmed their spherical morphologies (Figure 1.1) with diameters ≤200 nm.

Parallel to early reports,[10,11] our assembly method was expected to result in a high density of tosyl groups on the hydrophilic surfaces of the PNPs assembled from $\mathbf{1}_{35}-b-\mathbf{2}_{15}$ that could be used for bioconjugation. Exposing our surface-tosylated PNPs to oligonucleotide sequences containing 5′-terminal amine moieties led to the surface incorporation of single-stranded DNA. The presence of DNA on the PNPs was visually confirmed by TEM (Figure 1.4a) through hybridization with 13 nm gold nanoparticle (GNP) probes functionalized with complementary DNA sequences.[12]

Treating our parent tosylated PNPs with the same GNP probes (Figure 1.2) and our DNA-functionalized PNPs with noncomplementary GNP probes (Figure S1 in Supporting Information) revealed minimal nonspecific GNP−PNP interactions under identical experimental conditions. Further confirmation of duplex DNA formation between our DNA-functionalized PNPs and the GNP probes was obtained by UV−vis spectroscopy. By monitoring the absorbance of single-stranded DNA (λ_{max} = 260 nm) as a function of temperature, the thermal denaturation (transition from duplex to single-stranded DNA)[13] of the PNP−GNP probe assembly was observed (Figure S2A in Supporting Information). This same melting transition was observed by monitoring the surface plasmon absorption of nonaggregated GNPs (λ_{max} = 520 nm) over the same temperature range (Figure S2B in Supporting Information), confirming close packing of GNP probe particles on the PNP surfaces at hybridization.[14]

As antibodies often possess exposed nucleophiles, such as lysine residues and terminal amines, they should also be reactive toward tosyl-bearing materials. Thus, we prepared immunoconjugated PNPs by incubating aqueous suspensions of our tosylated PNPs with anti-

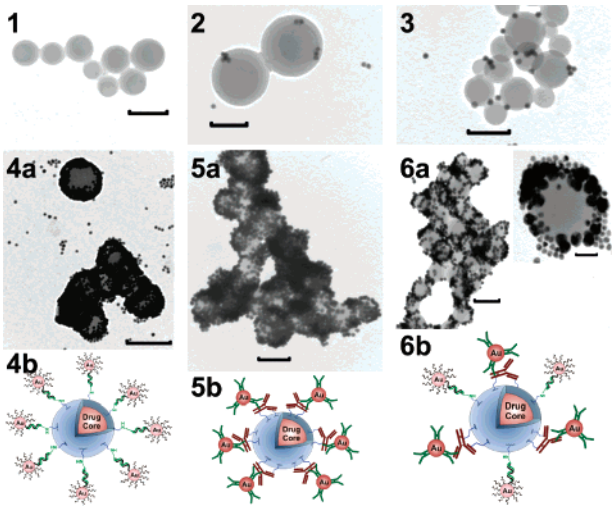

Figure 1. TEM images of (1) tosylated PNPs prepared from $\mathbf{1}_{35}-b-\mathbf{2}_{15}$; (2) tosylated PNPs incubated with 13 nm DNA-functionalized GNP probes; (3) tosylated PNPs incubated with 30 nm anti-IgY-functionalized GNP probes; (4a) DNA-functionalized PNPs hybridized to 13 nm GNP probes functionalized with the complementary sequences; (5a) anti-HER-2 IgY-functionalized PNPs binding to 30 nm anti-IgY-functionalized GNP probes; and (6a) Bcl-2 asODN- and anti-HER-2 IgY-functionalized PNPs as detected by the complementary DNA-functionalized 13 nm GNP probes and anti-IgY-functionalized 30 nm GNP probes. (4b−6b) Schematic illustration of 4a−6a, respectively. Images are shown on the same scale (bar = 200 nm), except for 2 (bar = 100 nm) and the inset in image 6a (bar = 50 nm).

Scheme 1. Preparation of Multifunctional PNPs from $\mathbf{1}_{35}-b-\mathbf{2}_{15}$

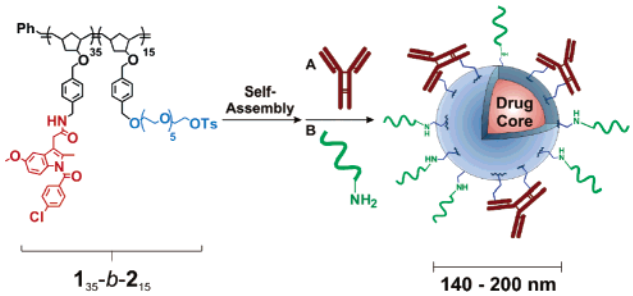

[†] Department of Chemistry and International Institute for Nanotechnology.
[‡] Biological Imaging Facility and Department of Neurobiology and Physiology.

10.1021/ja056378k CCC: $33.50

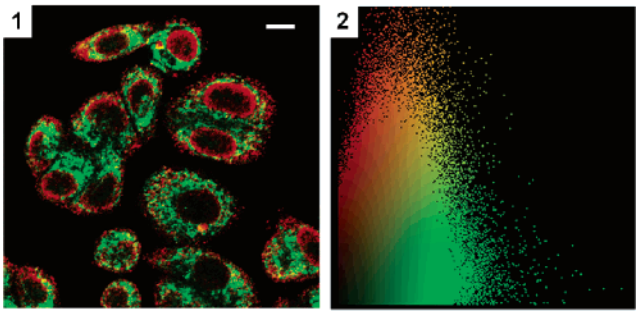

Figure 2. (1) Confocal laser-scanning microscopic image of SKBR3 cells incubated with PNPs that have been functionalized with fluorescein-dT-labeled Bcl-2 asODNs and anti-HER-2 IgYs. The cells were treated with goat anti-IgY labeled with Cy3 (red) prior to observation. (2) Scatter plot of colocalization for green and red channels generated from image (1), suggesting effective internalization of both DNA and antibodies bound to the PNPs (Pearson's correlation = 0.59; overlap coefficient $r = 0.73$).

HER-2 IgY. To confirm the presence of surface-immobilized anti-HER-2 antibodies on our PNPs, we exposed them to 30 nm GNP probes that were conjugated to anti-IgY secondary antibodies. The highly specific antibody-mediated PNP−GNP binding event was observable by TEM (Figure 1.5a). Control experiments revealed minimal nonspecific binding (Figure 1.3; see also Supporting Information), confirming that antibody−antibody interactions were indeed responsible for the observed PNP−GNP recognition.

PNPs functionalized with both antibodies and asODNs were prepared by parallel incubation of anti-HER-2 IgY and Bcl-2 asODNs with the tosylated PNPs. Visualization of the immobilized antibodies and asODNs on the resultant particles was accomplished with anti-IgY-functionalized GNP probes (30 nm) and complementary DNA-functionalized GNP probes (13 nm), respectively (vide supra). As shown in Figure 1.6a, both GNP probes bind specifically to the PNP surfaces, indicating simultaneous functionalization of our PNPs with antibodies and oligonucleotides. Most strikingly, this image provides direct visual confirmation of an orthogonal hierarchical assembly strategy using biopolymer-functionalized PNPs as scaffolds.

To evaluate cellular uptake of our multifunctional PNPs in vitro, we incubated them with SKBR3 human breast carcinoma cells that are known to overexpress the HER-2/*neu* gene products and internalize[15] antibodies raised against HER-2. In control experiments where SKBR3 cells were incubated with either fluorescein-labeled Bcl-2 asODN single strands or the corresponding DNA-functionalized PNPs lacking anti-HER-2 antibodies, only background fluorescence signal inside the cells was obtained after 16 h (Figure S4 in Supporting Information). By contrast, SKBR3 cells incubated for 16 h with multifunctional PNPs containing both anti-HER-2 IgY and fluorescein-labeled Bcl-2 asODNs exhibited significant colocalized cytoplasmic fluorescence after being stained with red-labeled anti-IgY, suggesting that surface-immobilized anti-HER-2 IgY effectively facilitates the internalization of our multifunctional PNPs (Figure 2).

In conclusion, ROMP-based amphiphilic block copolymers containing small-molecule drug segments and tosylated hexaethylene glycol segments were assembled into core−shell PNPs that allowed for the surface conjugation of DNA and tumor-targeting antibodies. These multifunctional PNPs were readily internalized in breast cancer cells that overexpressed the corresponding antigens. In light of the functional group tolerance of ROMP and our previous studies utilizing other chemotherapeutic drugs, the potential generality of this methodology for constructing PNPs that incorporate a range of bioactive agents with unique and potentially synergistic functions is immediately evident.

Acknowledgment. Financial support by the NIH through a CCNE grant, the AFOSR (PECASE Grant F49620-01-1-0303), NSF (DMR-CAREER Grant 0094347), the Packard Foundation, the NU Institute for BioNanotechnology in Medicine (IBNAM), Baxter Healthcare, Inc., and Robert H. Lurie Comprehensive Cancer Center is appreciated. S.T.N. is an Alfred P. Sloan research fellow. C.A.M. is grateful for an NIH Director's Pioneer Award, and acknowledges additional support from the NU NSF-NSEC and the AFOSR. We acknowledge the use of instruments in the Keck Biophysics Facility and the EPIC facility of the NU*ANCE* Center (supported by NSF-NSEC, NSF-MRSEC, Keck Foundation, the State of Illinois, and Northwestern University) at Northwestern University. We thank Prof. Robert Lamb, Dr. Reay Paterson, and Ms. Olga Rozhok (Northwestern University) for helpful discussions and use of cell culture facilities.

Supporting Information Available: Synthetic and preparative procedures for polymers and PNPs, characterization data, visualization protocols and data from cell studies, supplemental figures, and schemes are available. This material is available free of charge via the Internet at http://pubs.acs.org.

References

(1) Katz, E.; Willner, I. *Angew. Chem., Int. Ed.* **2004**, *43*, 6042−6108.
(2) Zhang, S. *Nat. Biotechnol.* **2003**, *21*, 1171−1178.
(3) Langer, R.; Tirrell, D. A. *Nature* **2004**, *428*, 487−492.
(4) Duncan, R. *Nat. Rev. Drug Discovery* **2003**, *2*, 347−360.
(5) Allen, T. M. *Nat. Rev. Cancer* **2002**, *2*, 750−763.
(6) Twaites, B.; de las Heras Alcarün, C.; Alexander, C. *J. Mater. Chem.* **2005**, *15*, 441−455.
(7) (a) Ferrari, M. *Nat. Rev. Cancer* **2005**, *5*, 161−171. (b) Service, R. F. *Science* **2005**, *310*, 1132−1134.
(8) (a) Cory, S.; Adams, J. M. *Nat. Rev. Cancer* **2002**, *2*, 647−656. (b) Hussaina, M.; Shchepinovc, M. S.; Sohailc, M.; Bentera, I. F.; Hollinsa, A. J.; Southernc, E. M.; Akhtar, S. *J. Controlled Release* **2004**, *99*, 139−155.
(9) (a) Olayioye, M. A.; Neve, R. M.; Lane, H. A.; Hynes, N. E. *EMBO J.* **2000**, *19*, 3159−3167. (b) Slamon, D. J.; et al. *Science* **1989**, *244*, 707−712.
(10) Bertin, P. A.; Watson, K. J.; Nguyen, S. T. *Macromolecules* **2004**, *37*, 8364−8372.
(11) Bertin, P. A.; Smith, D.; Nguyen, S. T. *Chem. Commun.* **2005**, *30*, 3793−3795.
(12) Storhoff, J. J.; Elghanian, R.; Mucic, R. C.; Mirkin, C. A.; Letsinger, R. L. *J. Am. Chem.* Soc. **1998**, *120*, 1959−1964.
(13) Marky, L. A.; Breslauer, K. J. *Biopolymers* **1987**, *26*, 1601−1620.
(14) Elghanian, R.; Storhoff, J. J.; Mucic, R. C.; Letsinger, R. L.; Mirkin, C. A. *Science* **1997**, *277*, 1078−1081.
(15) Austin, C. D.; Mazière, A. M. D.; Pisacane, P. I.; von Dijk, S. M.; Eigenbrot, C.; Sliwkowski, M. X.; Klumperman, J.; Scheller, R. H. *Mol. Biol. Cell* **2004**, *15*, 5268−5282.

JA056378K